TTK4210 Advanced Control of Industrial Systems, Exercise 6

Kristian Løvland

Contents

1 Abstract

In this project, a model of a butane distillation column was used to design a controller for the composition of two product streams consisting of n-butane and iso-butane, respectively. By identifying characteristics of relevant subsystems, PI controllers for the states of these systems were designed with the ultimate goal of keeping the purity of the products at a satisfactory level.

2 Introduction

A good introduction to the control problem we're faced with is given in the assignment text [1]. A short summary follows

The top product is required to contain no more than 4% n-butane, while the bottom product is required to contain less than 2,5% iso-butane.

These compositions, denoted x_D^* and x_B^* are in practice controlled through their temperatures. These are measured on the top and bottom of the distillation column, and are denoted T_D and T_B. The temperature needed to acheive the required compositions are shown in **??**, together with the actual temperature setpoint. These are a bit lower/higher than they strictly need to introduce a safety margin.

	Required temperature	Temperature setpoint
Top product (D)	$35,85°$ C	$35,30°$ C
Bottom product (B)	$47,69°$ C	$48,51°$ C

Table 1: Temperatures giving satisfactory product quality

To satisfy these specifications, the rest of the systems need to work well too. The levels M_D and in the top accumulator and M_B in the distillation column need to be controlled to stable setpoints. The same goes for distillation column pressure p.

To control these five variables, five degrees of freedom is needed. Our five manipulated variables are flow rates in different parts of the system, denoted V_T, L, D, V and B. Each of these is controlled directly by a valve.

Sjekk om dette stemmer

Table 2 shows the pairing of manipulated and controlled variables. As mentioned, it is assumed that choosing good setpoints for T_D and T_B gives satisfactory product quality. This control structure is called LV-control, after the manipulated variables used to control product quality.

Manipulated Variable	V_T	D	B	L	V
Controlled variable	p	M_D	M_B	T_D	T_B

Table 2: Variable pairings

3 Tuning secondary controllers

The secondary controllers were tuned individually using the SIMC method for PI controllers. A step in process input with an amplitude small enough to not cause problems (usually meaning 50% of maximum accepted input magnitude) in other parts of the system was used for all the secondary controllers, controlling the states D, L, B, V and p.

A summary of the method is given in [3]. The method assumes that the system can be approximated by a first order process with time delay

$$G(s) = \frac{ke^{-\theta s}}{1 + T_1 s} \tag{1}$$

and be controlled by a PI controller

$$K(s) = K_p \frac{1 + T_i s}{T_i s} \tag{2}$$

The SIMC method gives rules for choosing K_p and T_i, given a desired closed-loop time contant T_L. Assuming the step response behaves similarly to a first order system, the method is then as follows

1. Fit the step response to a first order model. This means finding time delay θ, slope $k' = \frac{dy/dt}{\Delta u}$ and time constant T_1 from the plot of the step response.

2. To achieve the desired time constant T_L, use the PI controller parameters $K_p = \frac{1}{k'} \frac{1}{\tau + T_L}$, $T_i = \min(T_1, 4(\tau + T_L))$.

The step experiments can be seen in figures 1, 3, 5, 7 and 9. The reference signals should have been omitted from these plots since we are dealing with open loop systems, and can safely be ignored here.

The plots show that for the first three variables, the accuracy of the simulation is clearly not sufficient for fitting a first order model (they behave in a stepwise fashion). Inspecting the order of magnitude of the gains and time constants may however still be useful. To approximate their sizes, a straight line was drawn from initial state to steady-state.

An attempt at making sense of these parameters is shown in table 3, together with the fitted values for V and p. This gives conservative estimates of k' and T_1.

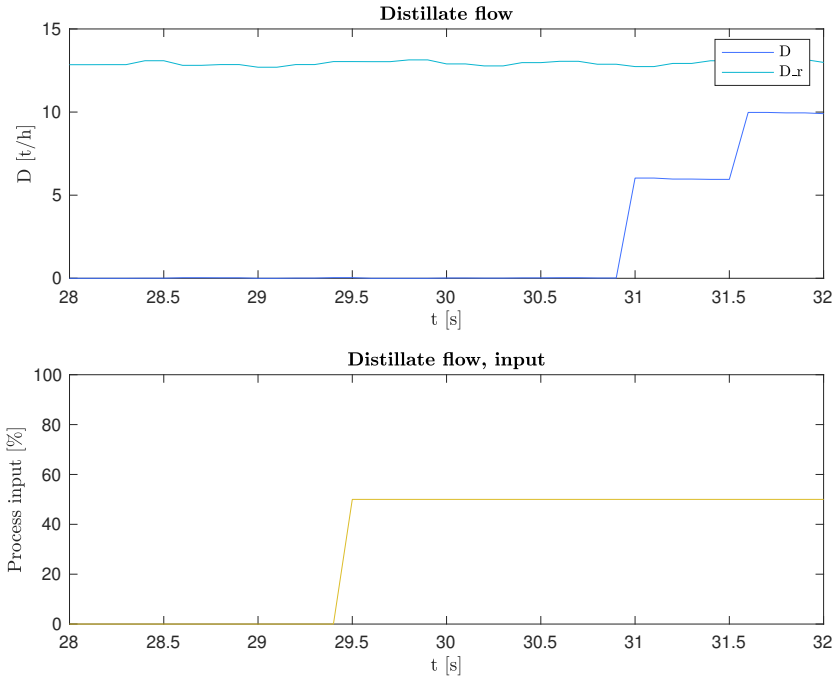

Fig. 1: Open-loop step response of D

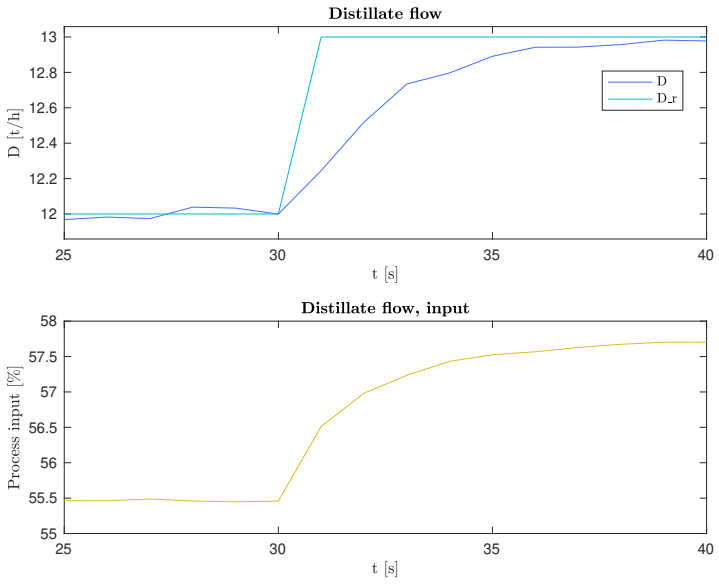

Fig. 2: Closed-loop step response of D

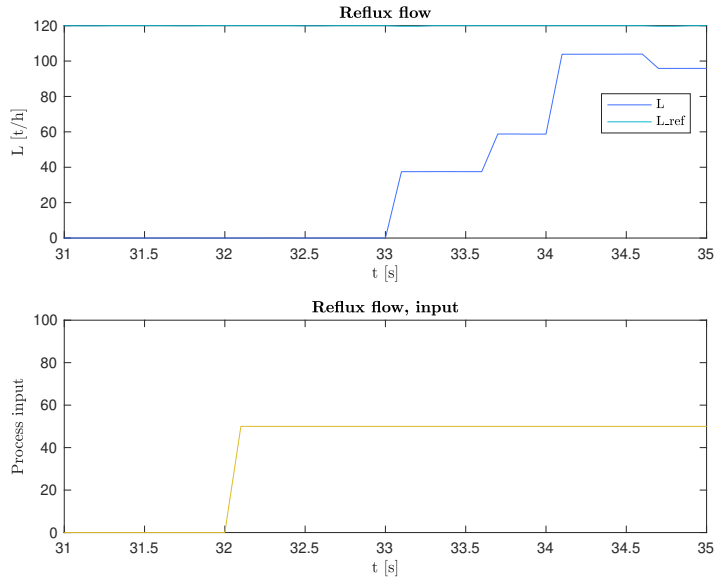

Fig. 3: Open-loop step response of L

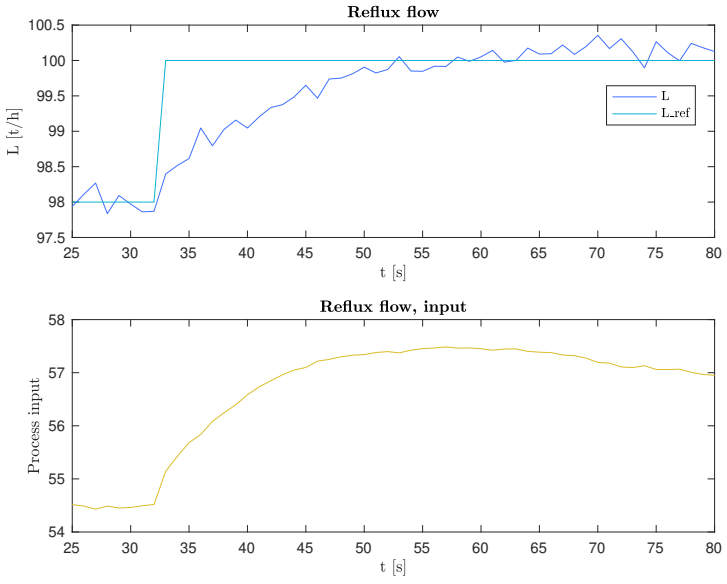

Fig. 4: Closed-loop step response of L

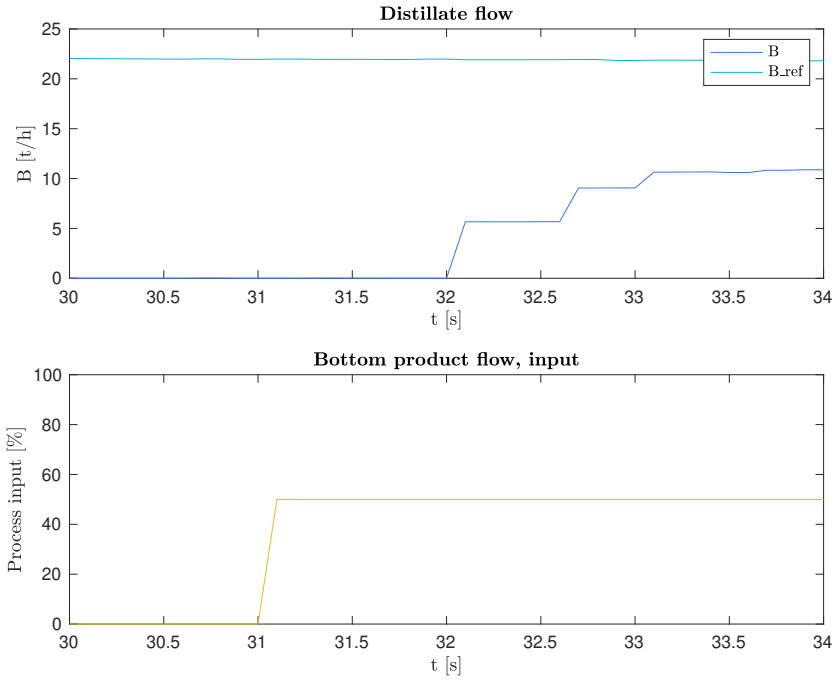

Fig. 5: Open-loop step response of B

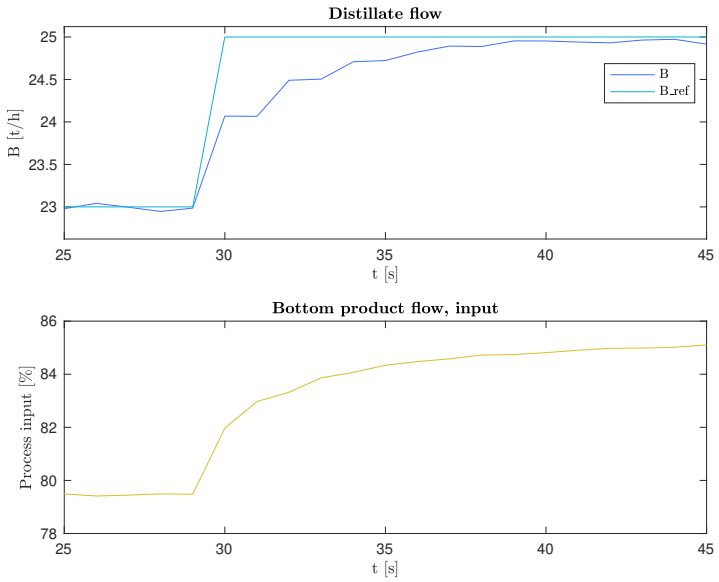

Fig. 6: Closed-loop step response of B

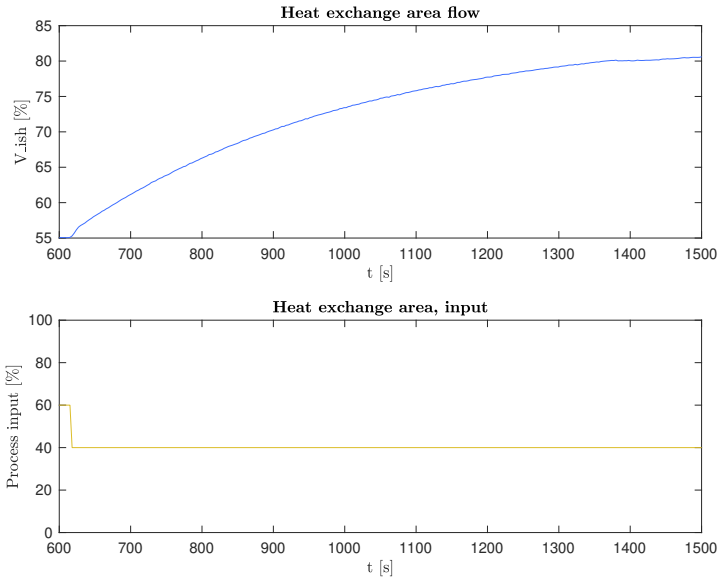

Fig. 7: Open-loop step response of heat exchanger area, related to V

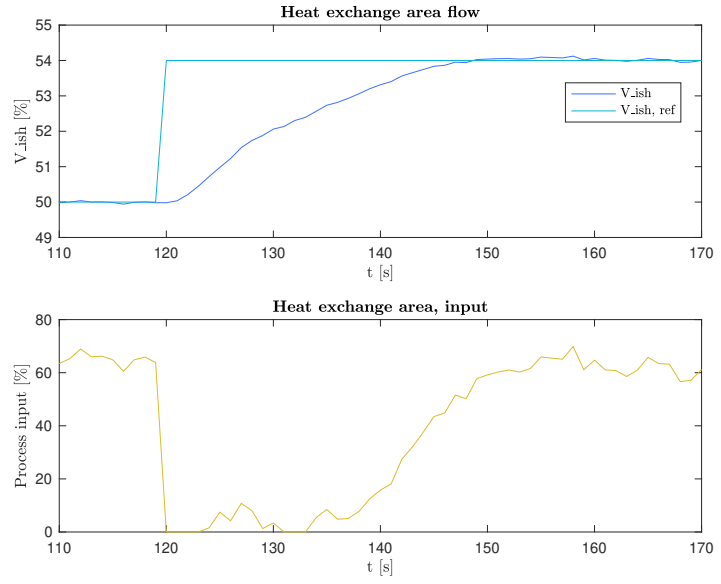

Fig. 8: Closed-loop step response of heat exchanger area, related to V

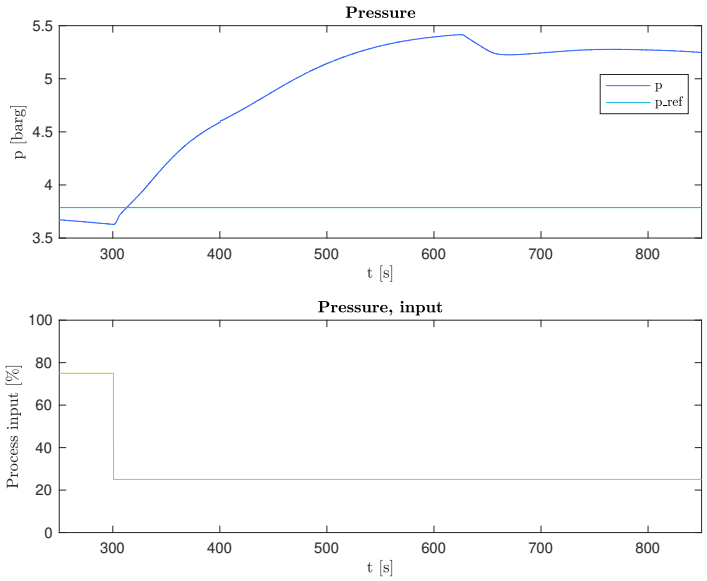

Fig. 9: Open-loop step response of p

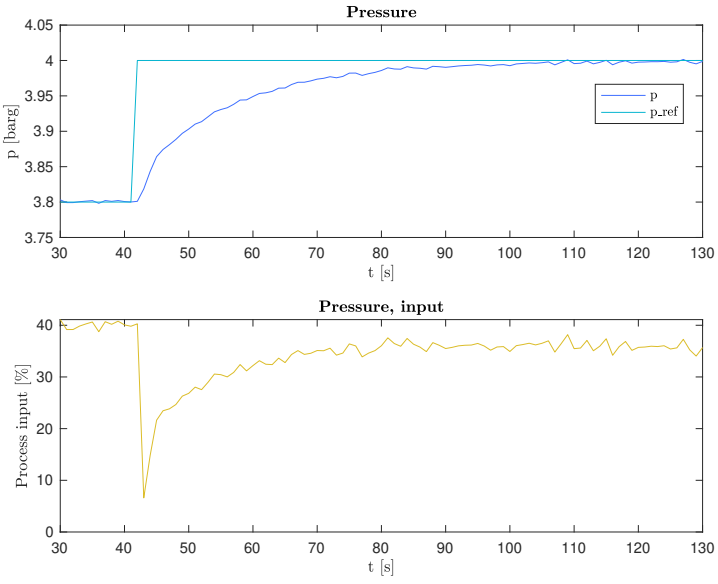

Fig. 10: Closed-loop step response of p

	τ	T_1	$\frac{dy}{dt}$	Δu	k'	T_L
D	1,0s	0,4s	14,3	50%	28,6	2s
L	1,0s	1,0s	47,5	50%	95,0	2s
B	1,0s	0,6s	10,0	50%	20,0	2s
V	≈ 0	400s	0,028	20%	0,14	10s
p	≈ 0	200s	0,088	50%	0,18	10s

Table 3: Identified parameters for inner loop

In the table, a desired time constant for the controlled system T_L is shown in the rightmost column. For a quick response, choosing $T_L = 0,3\tau$ is suggested in [**?**]. Some simple trial and error in K-spice showed that this lead to oscillation and unfortunate interaction between control loops, especially the controllers for D and L. This is probably partly due to the underestimates of k' and T_1 for these variables, since conservative estimates of these results in more aggressive controllers (to compensate for the slow system) when using the SIMC method.

Due to this unsatisfactory behaviour, $T_L = 2\tau$ was chosen for the three fastest control loops instead. The time delay was hard to make a meaningful reading of for the two other systems, so a somewhat arbitrary choice of $T_L = 10s$ was chosen for these systems (instead of using the $T_L = 2\tau$ rule). Like all the other parameters, these were not absolute choices, but a good starting point for further tuning.

After calculating the SIMC controller values some qualitative tuning using K-spice simulations was, not surprisingly, needed. For D and L, the integral times were kept fixed, and the gain was decreased to avoid oscillations. For B, it was necessary to reduce the integral time in addition to reducing the gain to avoid oscillation. The response of V was slow, and to avoid bandwith limitations in the control of T_B later, both controller parameters were changed to give dramatically more aggressive behaviour. For p, the stationary deviation was initially removed pretty slowly, so the integral time was reduced, while also reducing gain to avoid oscillation.

The results of implementing these controllers in K-spice, using the internally scaled gain $G = K_p \frac{(y_{\max} - y_{\min})}{(u_{\max} - u_{\min})}$ for all controllers, are shown in figures 2, 4, 6, 8 and 10.

Sørg for å få p skalert riktig (enhet er trykk, ikke flow)

	$K_{p,\text{SIMC}}$	$T_{i,\text{SIMC}}$	$K_{p,\text{final}}$	$T_{i,\text{final}}$
D	0,012	0,4s	0,0035	0,4s
L	0,035	1,0s	0,0018	1,0s
B	0,016	0,6s	0,0025	1,0s
V	0,71	40s	1,65	10s
p	0,57	40s	0,25	20s

Table 4: PI controller parameters for inner loop

4 Level controllers

In this section, the subsystem consisting of the levels in the reflux drum and distillation column is identified, using the inputs D and B. Let $y = [M_D \quad M_B]^T$ and $r = [M_{D,\text{ref}} \quad M_{B,\text{ref}}]^T$. By exciting the controlled system

$$y(s) = L(s)e(s) = G(s)K(s)(y(s) - r(s)) \tag{3}$$

with changes in the reference r, the loop transfer function $L(s) = \frac{y}{e}(s)$ may be identified. Choosing $K(s)$ to be diagonal makes further analysis and controller tuning easier.

4.1 System identification and analysis

4.1.1 Experiment

The level controllers in the distillation column and reflux drum were expected to be more or less independent, but a MIMO experiment followed by identification using the `d-sr` toolbox was used anyway, due to the convenience of being able to reuse code in the composition control task. The system was excited by step changes in references for M_D and M_B, which were controlled with P controllers, both with $K_p = 1200$. The references were changed after different intervals, to better extract information about all frequencies. The states were attempted held in a reasonable interval, to avoid nonlinear effects such as saturation. The experiments are shown in figures 11 and 12.

4.1.2 Analysis

The identified model was chosen to have order 2, which is natural for a what was expected to be a diagonal system with two variables. The interactions

of the resulting system is shown in figure 13, which show the RGA of the identified $G(s)$. Inspecting this plot shows that the magnitudes of the off-diagonal elements are negligible at frequencies above $10^{-3}\frac{\text{rad}}{\text{s}}$. The diagonal elements have gain close to unity at the bandwith frequency (which is around $\omega = 0,01$). Since interaction is low, a diagonal controller

$$K(s) = \begin{bmatrix} k_1(s) & 0 \\ 0 & k_2(s) \end{bmatrix} \tag{4}$$

with PI controllers $k_1(s)$ and $k_2(s)$ may be designed independently based on the diagonal elements in the identified $G(s)$. In the following analysis, $L(s)$ is used for simplicity, since it is simply a scaled version of $G(s)$. The controller designed below will then simply be multiplied by the existing $K(s)$ when being implemented.

Figures 14 and 15 show the Bode plots of the transfer functions in the diagonals of the identified model. Ignoring the360° error in phase, the gain margin of loop transfer function $l_{11}(s) = \frac{M_D}{M_{D,ref}}(s)$ may be found to be to be 6,74dB as $\omega \to \infty$. Likewise, the gain margin of $l_{22}(s) = \frac{M_B}{M_{B,ref}}(s)$ is read to be 10,7dB as $\omega \to \infty$. Using the 6dB gain margin rule of thumb (which is often used in [3]), $K_{p,D}$ should not be increased by any significant amount, while $K_{p,B}$ might be increased by a factor of $10^{(10,7-6)/20} \approx 1,7$, yielding the controller gain $K_{p,B} = 2000$.

The phase plot of l_{11} shows that the integral controller should be active in the lower frequency spectrum. To avoid the phase crossing the $-180°$ line, the inequality $\frac{1}{T_{i,D}} < 2 \cdot 10^{-4}$ should be respected. Choosing $T_i = 5000s$ satisfies this. The phase response of l_{22} is pretty similar to the one of l_{11}, so initially choosing the same integral time for control of M_B should be reasonable.

Figures 16 and 17 shows the magnitudes of the sensitivity functions for the two systems using these controllers. The distillation column is, not surprisingly, the hardest system of the two to control quickly. One might wish to push the bandwith of the M_B loop further to the right, but inspecting the phase plot again suggests not to attempt this. This is because the phase margin would be dangerously low K_p was increased or T_i was decreased, and the system would become more sensitive to time delays and similar phenomena. Disturbances at frequencies above $0,005\frac{\text{rad}}{\text{s}}$ should hopefully not be common in this system anyway.

Figur av stegrespons til nivåregulering

.

Dette er teknisk sett trans-fer-funksjon fra feil til til-

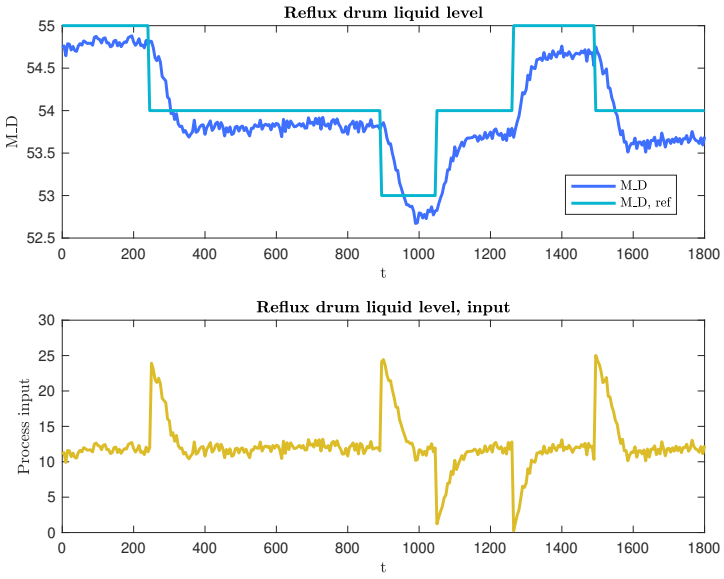

Fig. 11: System identification experiment for M_D controller

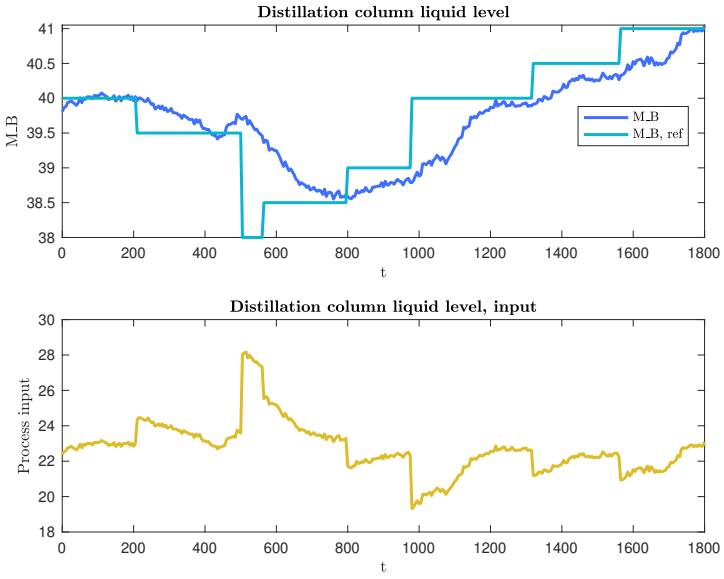

Fig. 12: System identification experiment for M_B controller

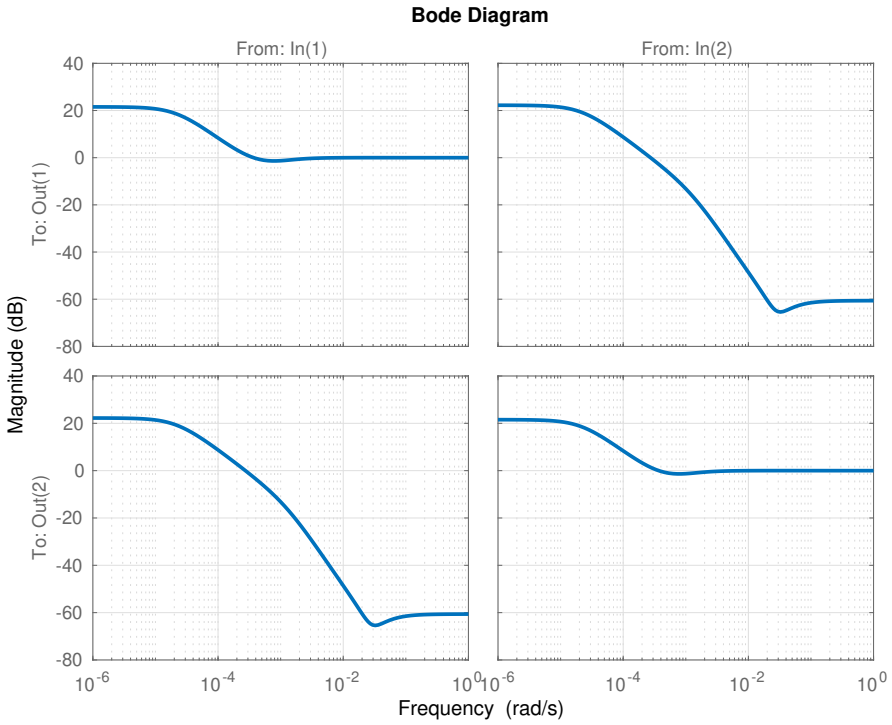

Fig. 13: Magnitude of RGA of identified BD system

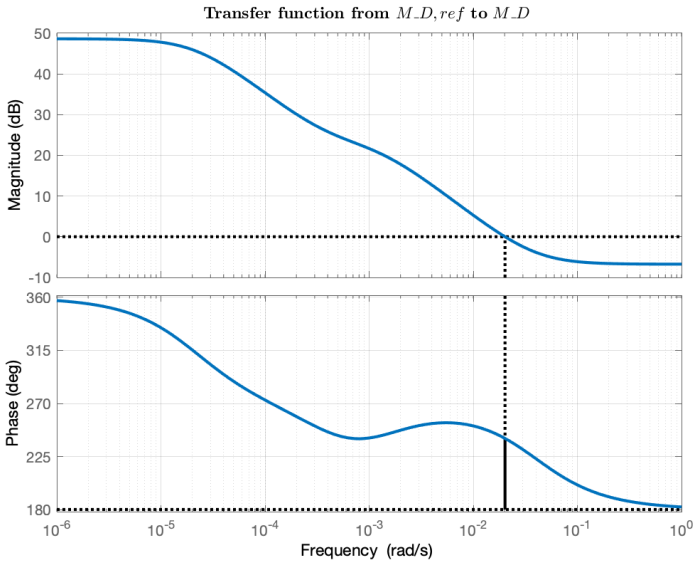

Fig. 14: Magnitude and phase response of reflux drum level from reflux drum level reference

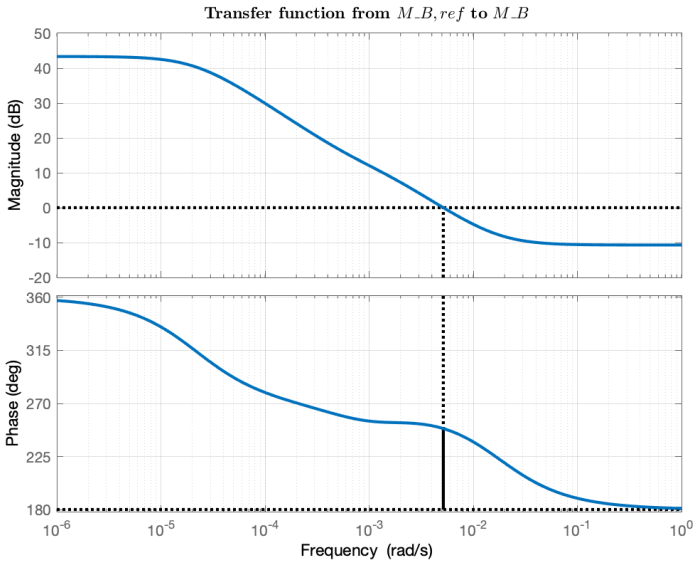

Fig. 15: Magnitude and phase response of distillation column level from distillation column level reference

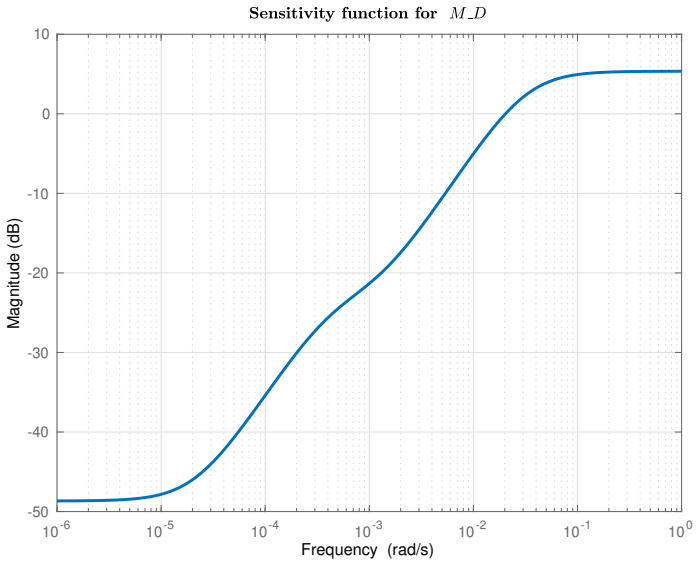

Fig. 16: Sensitivity function for reflux drum level control

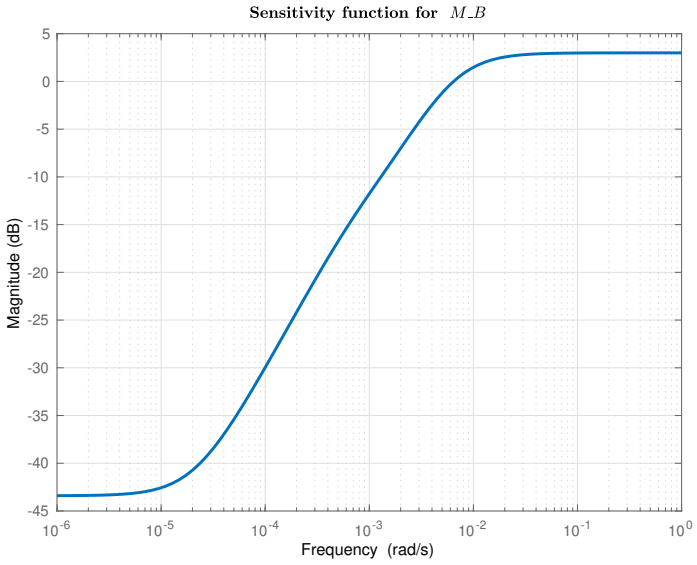

Fig. 17: Sensitivity function for distillation column level control

4.2 Controller tuning

Simulation in K-spice showed stationary deviation in M_D. To counteract this, the integral time was reduced. Control of M_B worked satisfactory using the PI controller derived from the frequency analysis above.

The initial parameters based on loop-shaping, and the final ones are shown in table 5.

	$K_{p,\text{initial}}$	$T_{i,\text{initial}}$	$K_{p,\text{final}}$	$T_{i,\text{final}}$
M_D	1200	5000s	1200	1000s
M_B	2000	5000s	2000	5000s

Table 5: Parameters for level controllers

5 Composition controllers

Let $y = [T_D \quad T_B]^T$, $r = [T_{D,\text{ref}} \quad T_{B,\text{ref}}]^T$ and $u = [L \quad V]^T$. By changing the setpoints for the manipulated variables L and V, the system transfer function

$$G(s) = \frac{y}{u}(s) \tag{5}$$

may be identified directly.

5.1 System identification and analysis

5.1.1 Experiment

Identification of the LV system was done in a similar manner as in the previous section, using step changes in input (but open-loop this time). Again, `d-sr` was used for identification. The periods of the step changes were chosen more systematically than in the level experiment, with periods of 5 minutes, 15 minutes and $\approx$ 2 minutes being used for different periods of time. This was done to get an accurate representation of the system at all frequencies. The inputs L and V were changed alternatingly (i.e. 90° out of phase), to avoid ambiguity in which input caused what effect. Figure 18 shows the experiment.

5.1.2 Analysis

Figure 19 shows the RGA of the identified system $G(s) = \frac{y}{u}(s)$. The chosen pairing is clearly the most reasonable. The interactions doesn't seem to be any problem, but the RGA doesn't tell the whole story. There is reason to believe that temperature in the bottom affects temperature in the top, and the right tool for this analysis is the *Performance Relative Gain Array* (PRGA).

Let $\tilde{G} = \text{diag}\{g_{ii}\}$, i.e. it contains only the diagonal elements of the system matrix. This matrix is a useful tool for analysing interactions, and is used in the definition of the PRGA

$$\Gamma = \tilde{G}G^{-1} \tag{6}$$

This matrix is used as a measure of interaction. It is scaling dependent, so before any further analysis is done, this has to be taken into account. Given a subsystem

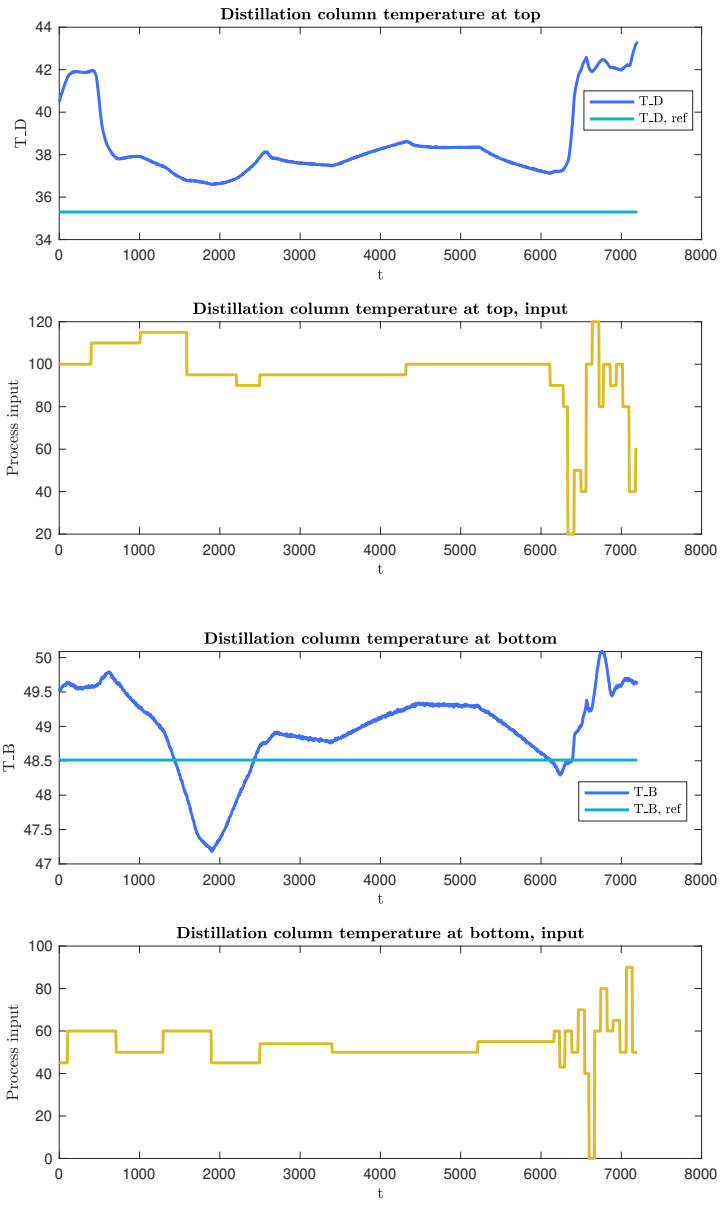

Fig. 18: Response of T_D and T_B to step changes in L and V

$$e = y - r = G(s)u + G_d(s)d - r \tag{7}$$

the signals should be scaled such that the maximum expected disturbance and maximum acceptable error both are of magnitude one. Table **??** shows the range used in K-spice for the states in the temperature control loops, and maximum accepted/expected value for signals only used in analysis (e and d). To be clear, the following analysis holds for both control loops, with y being temperature, r reference temperature, and u process input. The maximum error allowed is chosen based on the lowest margin proposed in the assignment text. The choice of a maximum disturbance of one degree celsius is somewhat arbitrary, but seemed reasonable and at least not too optimistic given the information that one degree is considered a large step in temperature.

The PRGA using this scaling is shown in figure 20. It is now clear that one can't simply choose a bandwith of $0,01\frac{\text{rad}}{\text{s}}$ and call it a day, since the interaction from V to T_D has its peak at this frequency.

What should be done, then? Since we're dealing with a MIMO system, only using the diagonal parts of G for designing controllers won't suffice. Our main objectives are to follow the reference, and to counteract disturbances. In [2], some rules for designing independent controllers for MIMO systems are proposed.

For effecient reference tracking in a SISO system, an error magnitude $|e(j\omega)|$ less than one is achieved when

$$|S(j\omega)R| < 1 \tag{8}$$

for reference changes of magnitude R, for all frequencies ω up to the maximum frequency ω_r where good reference tracking is required. More explicitly, this requirement can be stated as

$$|1 + L(j\omega)| > R \tag{9}$$

The situation for a MIMO system is a bit more complicated when we have interactions like shown above. This is where the PRGA is useful. It is shown in [2] that the MIMO analogue of equation 9 can be stated, using the PRGA, as

$$|1 + L_i| > |\gamma_{ij}| \cdot |R_j| \tag{10}$$

Here, $L_i = g_{ii}k_i$ is the loop transfer function in loop i, and R_j is the magnitude of the reference change in loop j. For simplicity, it is assumed that no disturbances of magnitude larger than the accepted error enters the system. This shouldn't be too restrictive, since disturbances in a system like this are either

1. Slowly varying, meaning the integral effect in the controllers take care of them

2. Due to measurement, meaning they enter well above the bandwith of the system

Assuming $R_1 = R_2 = 1$, the requirements are as plotted in figures 21 and 22, using $L_i = G_i$ (P controllers with unit gain). Inspecting these, it becomes clear that the state most desperately in need of control is T_D. This is not surprising, since the PRGA showed the effect of T_B on T_D being large, while the effect the other way was more or less negligible. Hence, suppressing the effects T_B has on T_D is our most important task, while the control of T_B should be pretty problem free if the controller parameters aren't completely ridiculous. To shape $|1 + L_1|$, the integral time was first changed. $T_i = 100$s turned out to give a low maximum distance between $|1 + L_1|$ and $|\gamma_{1i}|$. K_p was then chosen to be as small as possible while still satisfying the criterion, yielding $K_p = 12$. This actually satisfies the criterion at all frequencies, as shown in 23. The restriction of the T_B loop being located in a higher part of the frequency spectrum gave rise to the choice of $T_i = 1000s$ for this PI controller. A sneaking feeling that the PRGA might have underestimated the effects of T_D on T_B was the background for requiring $|1 + L_2| > |\gamma_{22}|$ for all $\omega < 10^{-2}$, which as shown in figure 24 is satisfied when $K_p = 25$. A summary of the resulting controller is shown in table 6

	K_p	T_i
T_D	12	100s
T_B	25	1000s

Table 6: Parameters for temperature controllers

Variable	Min	Max	Maximum magnitude
T_D	25°C	50°C	25°C
T_B	25°C	50°C	25°C
$T_{D,\text{ref}}$	25°C	50°C	25°C
$T_{B,\text{ref}}$	25°C	50°C	25°C
L	$0\frac{\text{t}}{\text{h}}$	$120\frac{\text{t}}{\text{h}}$	$120\frac{\text{t}}{\text{h}}$
V	0%	100%	100%
e	-	-	$0,55$°C
d	-	-	$1,0$°C

Table 7: Scaling used in LV system analysis

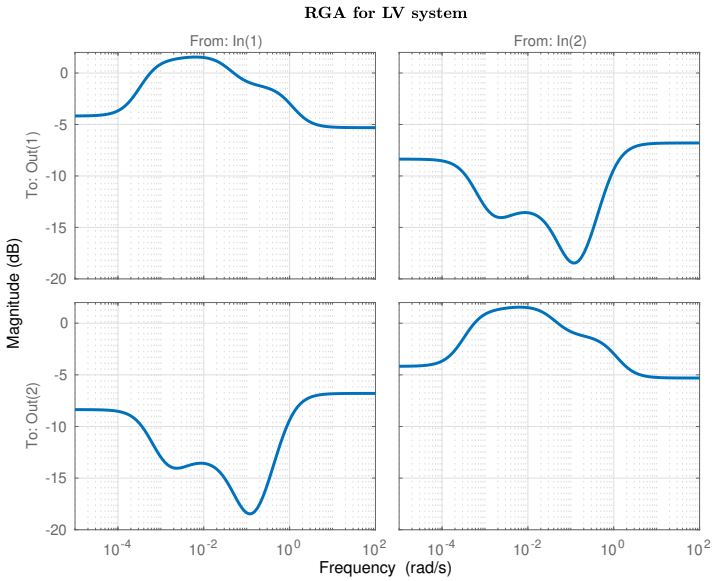

Fig. 19: RGA for LV system

5.2 Controller tuning

Using the given parameters results in the closed loop responses given in the following plots.

	K_p	G	T_i
D (FC1005)	0,0035	0,42	0,4s
L (FC1015)	0,0018	0,22	1,0s
B (FC1019)	0,0025	0,3	1,0s
V (LC1028)	200	200	10s
p (PC1024)	5	30	20s
M_D (LC1016)	1200	10	1000s
M_B (LC1015)	2000	16,7	5000s
T_D (TC1015)	12	2,5	100s
T_B (TC1088)	25	6,3	1000s

Table 8: Final controller parameters

6 Results

6.1 Plots

6.2 PI controller tuning

Table 8 shows the final PI controller parameters for all the control loops tuned in this project, also including the scaled gain G used in the K-spice implementation.

6.3 Reference tracking

References

[1] Morten Hovd, *TTK4210 Advanced Control of Industrial Processes, Assignment 6*, 2020.

[2] Sigurd Skogestad and Ian Postlethwaite, *Multivariable Feedback Control*, John Wiley & Sons Ltd, Chichester, 2nd edition, 2005.

[3] Jens G. Balchen, Trond Andresen and Bjarne A. Foss, *Reguleringsteknikk*, Institutt for Teknisk Kybernetikk, Trondheim, 6th edition, 2016.

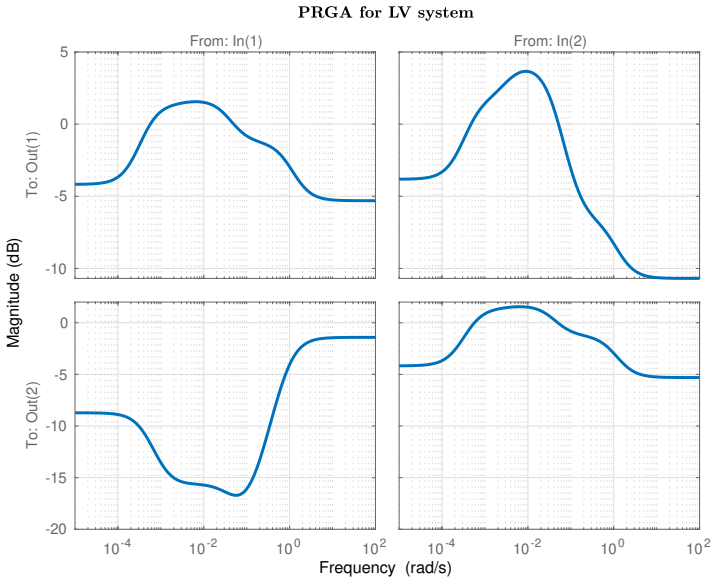

Fig. 20: PRGA for LV system

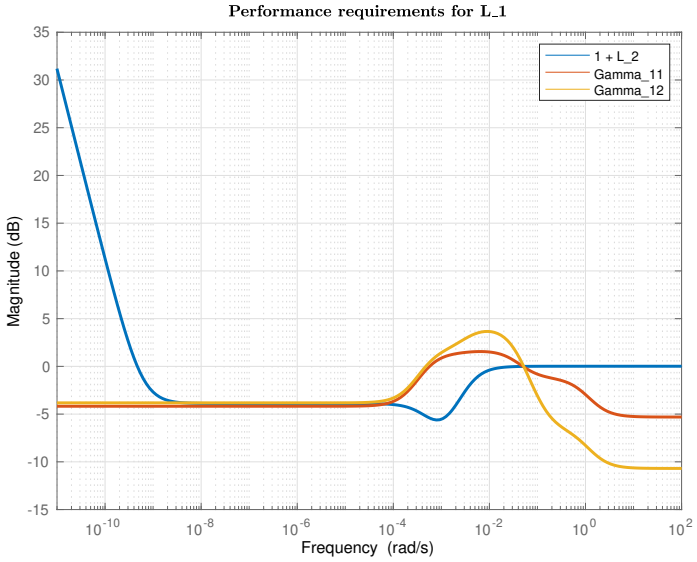
Performance requirements for L_1
1 + L_2
Gamma_11
Gamma_12
Magnitude (dB)
Frequency (rad/s)

Fig. 21

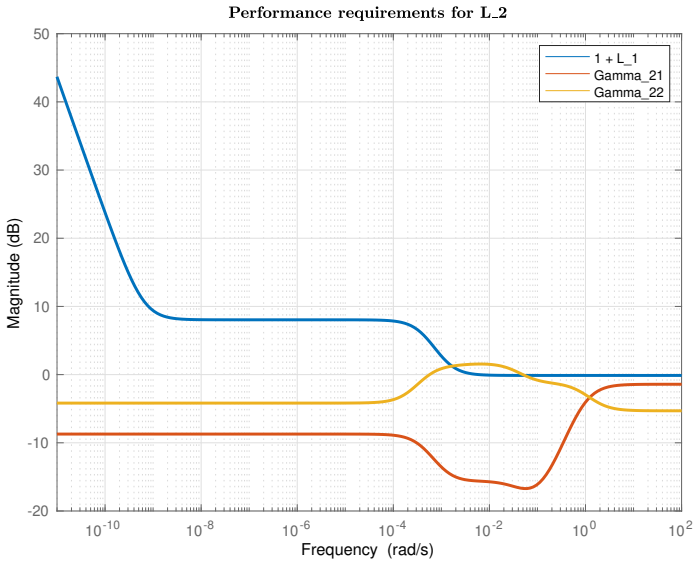
Performance requirements for L_2
1 + L_1
Gamma_21
Gamma_22
Magnitude (dB)
Frequency (rad/s)

Fig. 22

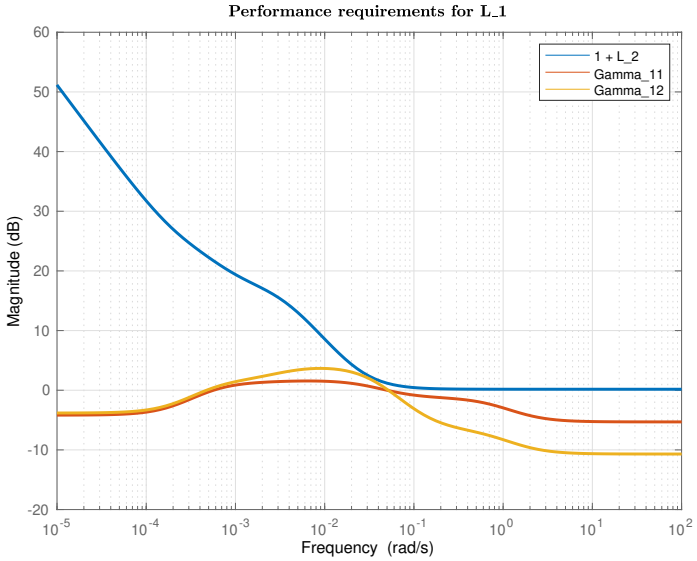
Performance requirements for L_1
1 + L_2
Gamma_11
Gamma_12
Magnitude (dB)
Frequency (rad/s)

Fig. 23

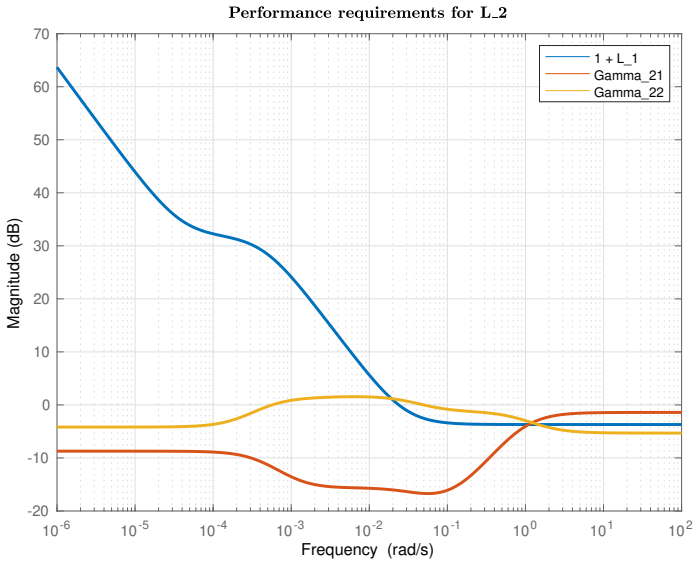
Performance requirements for L_2
1 + L_1
Gamma_21
Gamma_22
Magnitude (dB)
Frequency (rad/s)

Fig. 24

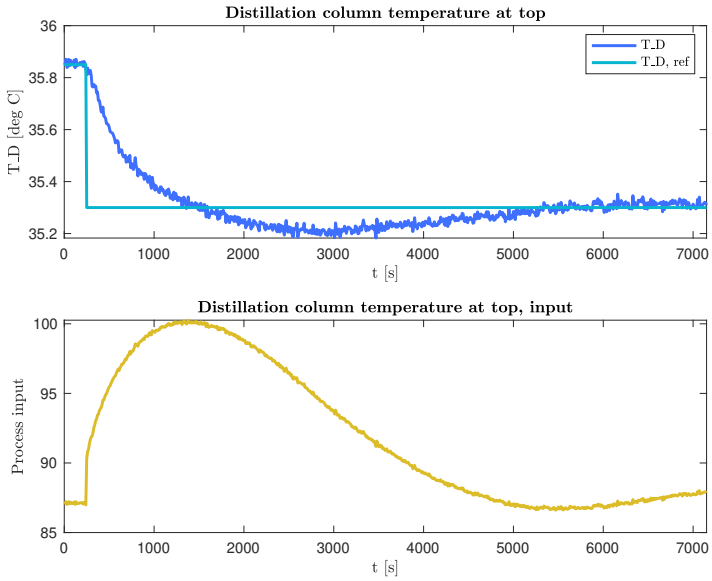

Fig. 25: Response of controlled T_D to step change in $T_{D,\text{ref}}$

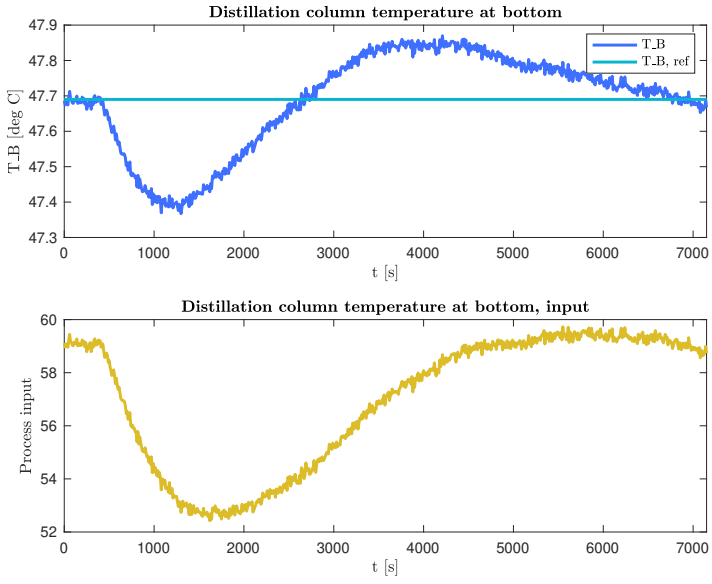

Fig. 26: Response of controlled T_B to step change in $T_{D,\text{ref}}$

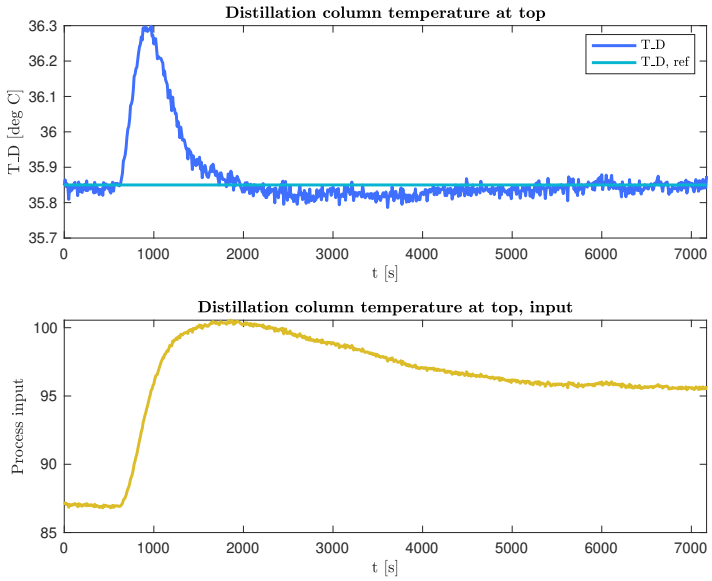

Fig. 27: Response of controlled T_D to step change in $T_{B,\text{ref}}$

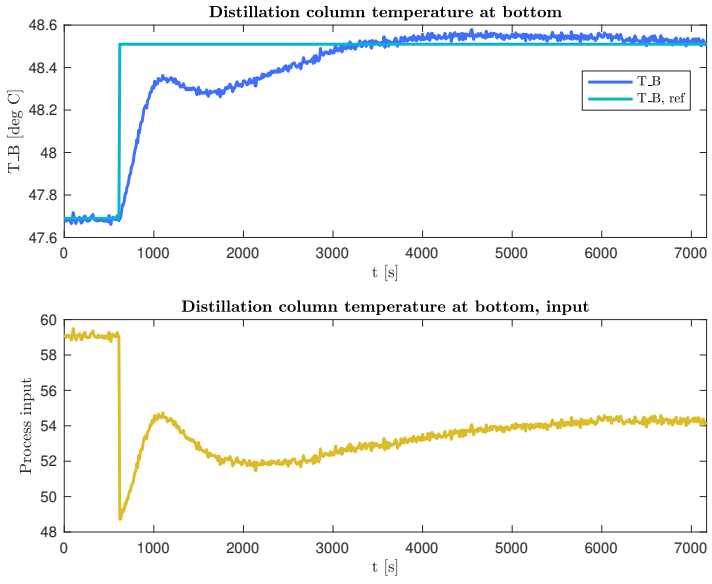

Fig. 28: Response of controlled T_B to step change in $T_{B,\text{ref}}$

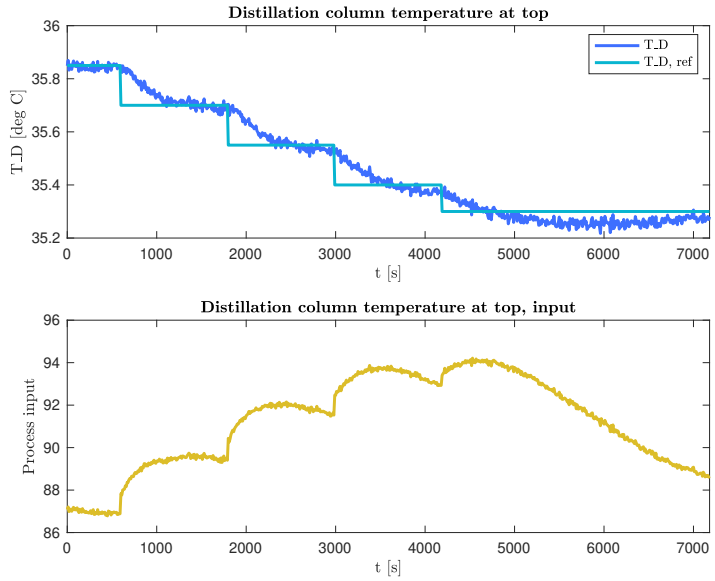

Fig. 29: Response of controlled T_D to stepwise step changes in $T_{D,\text{ref}}$

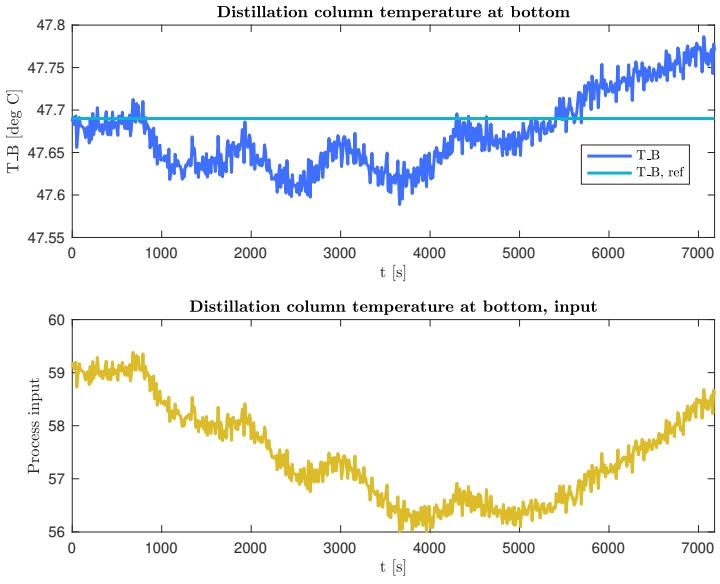

Fig. 30: Response of controlled T_B to stepwise step changes in $T_{D,\text{ref}}$

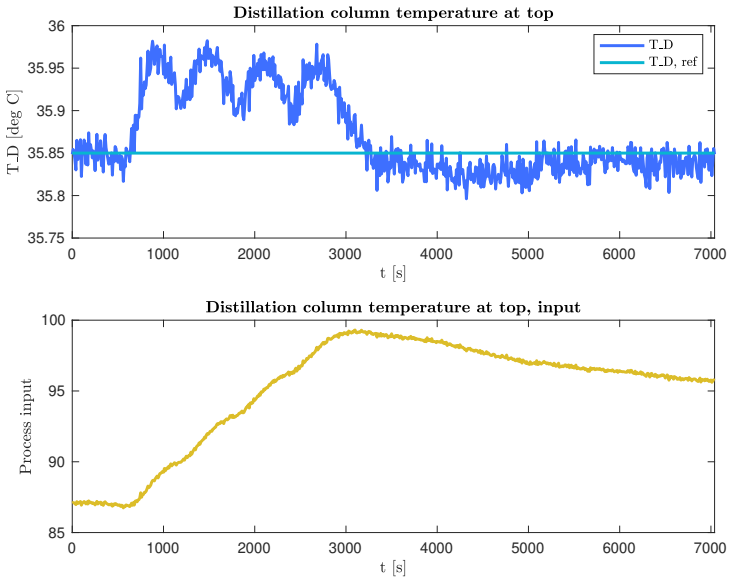

Fig. 31: Response of controlled T_D to stepwise step changes in $T_{B,\text{ref}}$

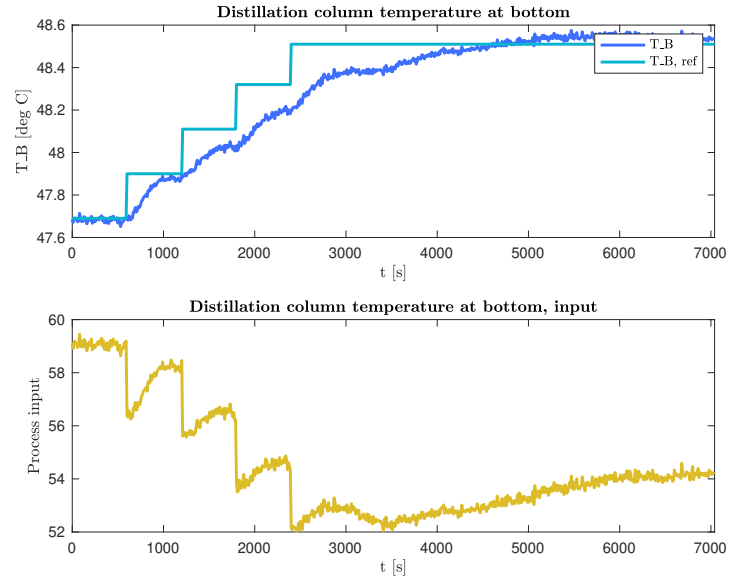

Fig. 32: Response of controlled T_B to stepwise step changes in $T_{B,\text{ref}}$